Fuel 302 (2021) 121129

Contents lists available at ScienceDirect

Fuel

journal homepage: www.elsevier.com/locate/fuel

Full Length Article

Response of crude oil deposited organic layers to brines of different salinity: An atomic force microscopy study on carbonate surfaces

Saravana Kumar [a,*], Ashit Rao [a], Mohammed B. Alotaibi [b], Subhash C. Ayirala [b], Ali A. Yousef [b], Igor Siretanu [a], Frieder Mugele [a]

[a] Physics of Complex Fluids Group and MESA+ Institute, Faculty of Science and Technology, University of Twente, P.O. Box 217, 7500 AE Enschede, The Netherlands
[b] The Exploration and Petroleum Engineering Center – Advanced Research Center (EXPEC ARC), Saudi Aramco, Dhahran 34465, Saudi Arabia

ARTICLE INFO

Keywords:
Improved oil recovery
Low-salinity effect
Polyaromatic hydrocarbons
Atomic force microscopy
Salting-out effects

ABSTRACT

The various microscopic processes that take place during enhanced oil-recovery upon injecting low salinity brines are quite complex, particularly for carbonate reservoirs. In this study, we characterize the in-situ microscopic responses of the organic layers deposited on flat Iceland spar calcite surface to brines of different salinity using Atomic force Microscopy (AFM). Organic layers were deposited from crude oil at the end of a two-step aging procedure. AFM topography images reveal that the organic layers remain stable in high-salinity brines and desorb upon exposure to low-salinity brines. In addition, the organic layers swell in low-salinity brines, and the stiffness of the organic layers is found to directly proportional to the brine salinity. These observations are explained in terms of 'salting-out' effects, where the affinity of organic layers to solvent molecules increases upon reducing the brine salinity. The swelling and desorption of organic materials provide access for the brine to mineral surface causing dissolution and change in wetting properties of the surface. Our results show the significance of de-stabilizing the organic layer on rock surfaces in order to design any successful improved oil recovery (IOR) strategy.

1. Introduction

Understanding the response of crude oil deposits on mineral surfaces when exposed to various brines is one of the key aspects of improved oil recovery (IOR) strategy that can ultimately lead to unravelling the physics underlying the low-salinity effect (LSE). Here, by LSE, we denote salinity dependent responses of the mineral-oil-brine interfaces that will lead to increased oil recovery upon injection of low-salinity brines into a porous mineral structure. Although indications of improved oil recovery by injecting low-salinity brines have existed since the 1960s [1], intensive research into LSE started in the 1990s [2–5]. This significant research effort has eventually led to a number of proposed mechanisms [6] for LSE such as multi-component ion exchange [7], mineral dissolution [8], fines migration [5], double layer expansion [9], salting-out effects [10], wettability-alteration to water-wet [8] and mixed-wet state [11], and changes in oil-brine interfacial properties [12]. But the actual physical interactions associated with these mechanisms for a given type of reservoir are still highly debated.

Enhancing oil recovery by LSE involves a hierarchy of processes ranging from molecular affinity between oil and the rock [13,14] over contact angle variations [15] on the pore scale [16–19] up to reservoir-scale two-phase flow phenomena [20]. All together, they determine the overall recovery factor. Individual mechanisms and their interplay do not transmit across length scales [21]. But often experimental data from a particular length scale are extrapolated to draw conclusions at other length scales. This may lead to correlations being misinterpreted as causal relations. Contradictions also arise from inconsistent definitions and notations. For example, across the IOR literature 'wettability alteration' is used for various physical phenomena such as changes in adhesion force between organic molecules and mineral surfaces [22], increased/reduced imbibition [23], changes in Amott index [24] and contact angle variations [25]. Despite the challenges of relating microscopic interfacial properties to macroscopic recovery, it is reasonably well-established from two-phase flow simulations [26] that reducing the water contact angle from very high to intermediate values, i.e. from strongly 'oil-wet' to intermediate-wet or water-wet conditions, does improve macroscopic recovery. Hence, searching for microscopic processes that reduce the water contact angle forms the basis of LSE-IOR

* Corresponding author.
E-mail address: saravana.kumar@utwente.nl (S. Kumar).

https://doi.org/10.1016/j.fuel.2021.121129
Received 2 February 2021; Received in revised form 21 May 2021; Accepted 23 May 2021
Available online 7 June 2021

research.

For sandstone reservoirs, a consensus has emerged that 'wettability-alteration' is the primary cause of LSE [2,6,27]. While it is clear that the mechanisms underlying LSE are different for sandstone and carbonate reservoirs [10,28], the latter is quite complex. Firstly, such complexity arises from the higher chemical activity of the carbonate surfaces coupled with the inherent heterogeneous reservoir conditions [29]. Secondly, the reactivity of carbonates is strongly dependent on temperature. And hence any effect of potential determining ions, sulfates, calcium, and magnesium on wettability alteration in carbonate reservoirs also becomes strongly dependent on temperature [30]. This taken together with the geothermal gradients that exist in the reservoirs makes it more complicated for carbonates than sandstone reservoirs.

The thermodynamic equilibrium established between crude oil (CRO), formation brine and minerals over geological time-scales leads to a complex configuration with an interfacial layer containing reconstructed carbonates, ions from the ambient brine, and interfacially active components of the CRO such as poly-aromatic hydrocarbons (PAH) [31]. This complex interfacial layer is responsible for the higher degree of oil-wetness as compared to bare calcite, which is intrinsically hydrophilic [31,32]. Several studies using rough rock material as a substrate (rather than e.g., flat calcite crystals) have also pointed out that such layers can be very heterogeneous leaving parts of the rock surface covered by trapped water rather than in direct contact with oil [16,17]. In the laboratory, researchers typically emulate this interfacial layer by subjecting originally clean surfaces to specific aging protocols. Note that not only the specific materials and their topography, but also the details of these protocols can have a substantial effect for both the absolute wettability and the response of interfacial layer to salinity variations of the injection brine [2,33]. Extraction of oil by water-flooding involves not only movement of the contact line, but also a disturbance of the responsive CRO-brine-mineral interfaces that can lead to degradation and dissolution of the interfacial layer and the underlying bulk mineral. Arguably, any improved oil recovery in low salinity water flooding ultimately originates from the perturbation of these interfacial layers. Therefore, understanding the perturbation response of the adsorbed organics and the mineral surfaces is important for the success of low-salinity IOR.

The type of organic component that gets adsorbed on to the mineral surface depends on the specific aging conditions. Nevertheless, poly-aromatic hydrocarbons such as asphaltenes and pre-asphaltenes are known to be a major class of organic components that gets adsorbed on to the mineral surface from crude oil [31,34–36] and form an integral part of the interfacial layer. Asphaltenes have been shown to exhibit changes in colloidal forces between them under different organic solvents [37,38] and simple salt solutions [39]. This results in changes of the morphology and mechanical properties of the asphaltene deposits [40]. Characterizing such changes can shed light on how low-salinity brines change the interactions among the crude-oil deposits and between the deposits and the mineral surface. Recently, researchers started to characterize the interfacial layer and its response to various brines in more detail at the micro- and nano-scale using a variety of techniques [16,17,31,32,36,41–43] such as scanning electron microscopy (SEM), confocal Raman spectroscopy, electron spectroscopy, mass spectrometry, microcomputed tomography, surface force apparatus, and atomic force microscopy (AFM). For example, on a mica substrate, Haagh et al. [33] showed that a slight change in the composition of the aging-brine during crude-oil aging changed the surface charge density of the crude oil deposits and also its macroscopic response to low-salinity brines. Chen et al. [41] characterized crude oil-brine-carbonate interactions using a variety of dynamic techniques. They found that the patchy interfacial ionic-organic layer readily detaches as flakes in low-salinity brines exposing the hydrophilic mineral surface. Ayirala et al. [44] reported the results from cryo-broad ion beam-scanning electron microscopy (cryo-BIB-SEM) to show the relatively less contact of crude oil with carbonate surface after flooding with low salinity brine. The microscopic contact-angles determined from high resolution SEM images in this study also showed lower water contact angles for low salinity brine when compared to the high salinity brine. Fenter et al. [45] studied calcite-petroleum interactions using X-ray reflectivity (XR) measurements and these results indicated that the presence of interfacial layer controls the properties of the interface. The interface is characterized by significant structural distortions with an increased surface roughness and is tightly bound to be displaced by aqueous brines.

Most of the microscopic characterization techniques work only ex-situ. Ex-situ measurements, by definition, do not take place in the native brine environment and are done only after some drying procedure. Such measurements do not have access to spatio-temporal phenomenon that happens under live environment which are the key aspects of microscopic characterization considered in the present study. Among the microscopic characterization tools that can be used in-situ, AFM is versatile with high lateral resolution which can be used not only to map the topography of a surface but can also be used to characterize material (phase imaging), mechanical properties and surface properties such as surface charge density.

In this work, we characterize the in-situ responses of aged calcite surfaces upon exposure to brines of variable salinity using various modes of Atomic Force Microscopy (AFM). We prepared CRO-brine-mineral interfaces by a previously established two-step aging protocol [31] involving exposure of freshly cleaved calcite surfaces to CRO-equilibrated formation water (FW) and equilibrated crude-oil at elevated temperatures for extended periods of time. We find that organic deposits (enriched in polyaromatic hydrocarbons) grown during aging form a coating that is relatively stable and protects the underlying mineral surface at high brine concentration. In low salinity environment, however, these deposits gradually soften and desorb. This exposes the underlying relatively water-wet calcite substrate to low-salinity brines leading to mineral dissolution.

2. Materials and methods

2.1. Materials

Iceland spar, obtained from Ward's Science, was cleaved mechanically to small pieces of a few cm^2 in surface area. 'Dead' crude oil, obtained from a carbonate reservoir, was used for the aging protocol. The SARA (Saturate, Aromatic, Resin and Asphaltene) analysis of the crude oil, carried out by a certified laboratory at Saybolt Nederland B.V., and summarized in Table S1, shows that the crude oil contains 2.6% of asphaltenes by mass. Formation water (FW) and high salinity water (HSW) were prepared by dissolving reagent grade salts (Sigma Aldrich) in milliQ water (18.2 mΩcm), stirred overnight and filtered using 0.2 μm polyether sulfone (PES) membrane. The composition of both FW and HSW can be found in Table S2. The composition of high-salinity brine (HSW) is similar to that of seawater. The dilutions of HSW (10xdil.HSW and 100xdil.HSW) are referred to as low-salinity brines in this study. Equilibrated crude oil (eqCRO) and equilibrated formation water (eqFW) were obtained by equilibrating equal volumes of FW and crude oil at 95 °C for 48 h. During this equilibration process, organic material of about 31 mg/l of humic acid equivalence (≈0.1 mM) from crude oil is transferred to FW [31]. Freshly cleaved calcite pieces were aged initially in eqFW for 16 h and subsequently in eqCRO for 7 days at 95 °C. The aged samples were then briefly washed with toluene to remove the excess oil layer. The samples that were aged only in eqFW were rinsed with milliQ water for 3–5 s to remove salt crystals and blown dry using pressurized nitrogen. A detailed description of the equilibration procedure and reservoir-pertinent fluids can be found elsewhere [31].

Atomic force microscope (AFM) imaging and force spectroscopy were done using a Bruker Dimension ICON instrument. The topography images were taken in dynamic amplitude-modulation mode whereas force spectroscopy was performed in static mode using Force Volume data acquisition technique. ScanAsyst-Fluid and OTESPA probes, from

Bruker, were used for both imaging and force spectroscopy. These probes are made of silicon and have nominal spring constant of about 0.7 N/m and 42 N/m, and a nominal tip radius of about 20 nm and 7 nm, respectively. The stiffness of the AFM cantilever (k_c) was calibrated via thermal tuning method [46]. Topography images were post-processed using Gwyddion software (version 2.55) and the force-distance curves from force spectroscopy data were analyzed using a house-built routine written in MATLAB. The topography images are of 512 × 512 resolution whereas the force volume maps are of either 256 × 256 or 100 × 100 resolution with 128 data points on each trace and retrace force curve.

2.2. Methods

All the imaging and mechanical characterization experiments were done at room temperature (22 °C) in-situ in the respective fluid environment, unless explicitly mentioned otherwise. The aged calcite samples were glued to a steel puck using Norland optical adhesive 81 (Norland Products, Inc.) and cured using UV-light. The samples were then placed in a petri dish containing the relevant brine (of volume 17 ml) and put under the AFM scanner. The sample was held in place by magnets under the petri dish. For eqCRO-aged samples, the aging procedure produces a heterogeneous distribution of material on the surface. The region with relatively more deposits (which can be seen as darker regions under optical microscope) was chosen to be probed using AFM (Fig. S1). Once a suitable area was found, its response was tracked continuously as function of time and brine composition. Fluid exchange of the brines (at least 3 cell volumes) was done using syringe pumps at the rate of 2 ml/min.

The topography images were corrected for imaging artefacts such as horizontal scars. Then the minimum point in the height was set to zero. To calculate the area covered by the deposits, a grain analysis method using a thresholding algorithm, in Gwyddion software, was used where a height criterion and a slope criterion (to identify edges of the deposits) were set. To obtain the stiffness of the sample from the force-distance curves, the sample and the cantilever were modeled as Hookean springs in series. As previously mentioned, the stiffness of the AFM cantilever is represented by k_c. The effective stiffness (k_{eff}) of the sample and the cantilever was obtained from the slope of a line fitted to approach force curve in the constant compliance region. The region of fit was chosen to be between 10% and 90% of the peak force in each curve. Then the stiffness of the sample (k_s) can be obtained as follows [47]:

$$k_s = \left(\frac{1}{k_{eff}} - \frac{1}{k_c}\right)^{-1} \quad (1)$$

3. Results

3.1. Initial aging

Fig. 1 shows typical calcite surfaces as used in the subsequent experiments and initial aging procedure that was developed before [31]. Freshly cleaved Iceland spar displays characteristic cleavage triangles with step heights of a few atomic layers, Fig. 1**a**. The flat terraces are covered by small hillocks (see inset) that arise from the reconstruction and roughening of calcite surfaces upon exposure to ambient humidity, see e.g. [48]. After 16 h equilibration with eqFW at 95 °C, the surfaces are covered with an almost uniform distribution of deposits (Fig. 1**b**). These deposits have well-defined shapes and an average diameter of about 45 nm (**Fig. S4**). They consist primarily of calcite with a small amount of Mg^{2+} (roughly 10 mol% $MgCO_3$; see **Figs. S5, S6** and [49]) and organics such as polyaromatic hydrocarbons (PAHs), as deduced previously from Energy-dispersive X-ray spectroscopy (EDX) and Raman spectroscopy [31]. This agrees well with the previously reported observations that the top calcite layer is reconstructed and composed of both inorganic and organic components [31,32,36,41]. This layer will henceforth be called modified calcite. After subsequent equilibration with eqCRO for 7 days at 95 °C, the samples become substantially rougher and display a heterogeneous distribution of aggregates on the surface (Fig. 1**c**). Despite the heterogeneous distribution, these aggregates show preferential adsorption on to macro-steps of the modified calcite (see Fig. 2). High energy surface features such as macro-steps are active sites for adsorption of organic aggregates [31,32]. These aggregates vary in shape and size from tens of nanometers to even micrometers (Fig. 1**c**). Our previous work shows that they are enriched in PAHs [31]. The Raman intensity for the PAHs (integrated in the range between 1230 cm^{-1} and 1745 cm^{-1}) is about 3 times higher for eqCRO-aged samples relative to eqFW-aged samples (**Fig. S5**). This indicates that the surface deposition of organic materials from eqCRO is

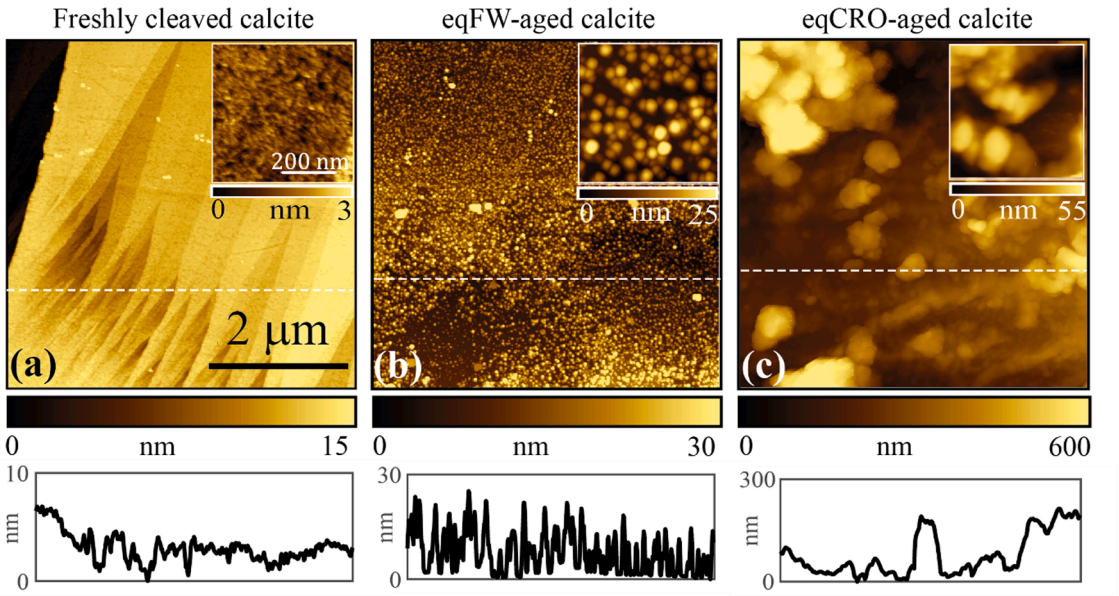

Fig. 1. Morphological evolution of calcite upon aging. Top row - Taping mode AFM topography images taken in air. Bottom row – cross-sections along dashed lines in images (note the different range of the vertical scales). (a) Freshly cleaved Iceland spar calcite. (b) Calcite surface after aging in eqFW for 16 h at 95 °C. (c) Calcite surface after subsequent aging in eqCRO for 7 days at 95 °C. The rms roughness values are 2.5, 5.5, 126 nm of the topography images in panels (a), (b), and (c) respectively. Insets: zoom into topography images. Scale bars in a) also apply to b) and c).

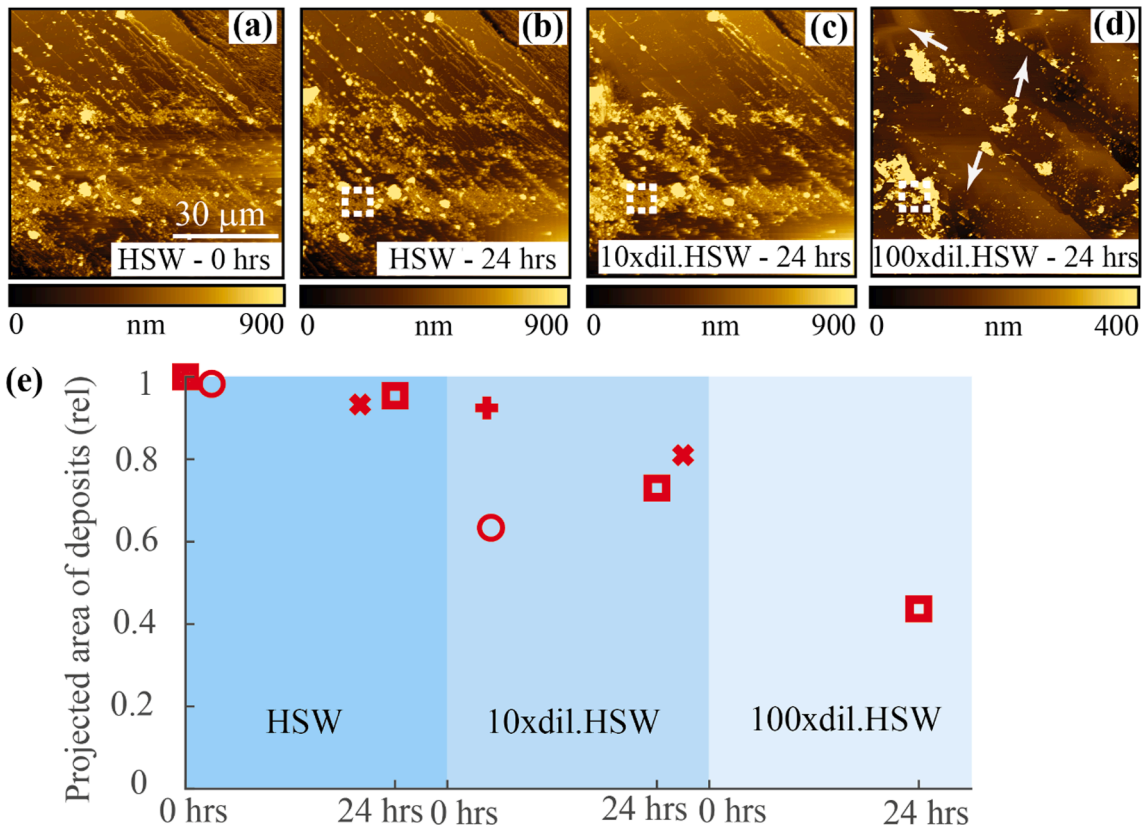

Fig. 2. In-situ AFM topography images of eqCRO-aged samples in various dilutions of HSW (a) initial exposure to HSW. (b) 24 h in HSW. (c) 24 h in 10xdiluted HSW (d) 24 h in 100xdiluted HSW. Note the removal of most organics and the appearance of characteristic etch pits (white arrows). (e) Projected area of organics normalized by the initial area in HSW for various brines. Red squares: panels (a)-(d) (see also **Fig. S7**). '+', 'o' and 'x' symbols: **Figs. S8–S10,** respectively. The error bars, for 10% uncertainty in the slope threshold for estimating area, are smaller than the symbols in panel (e) and hence not shown. (For interpretation of the references to colour in this figure legend, the reader is referred to the web version of this article.)

substantially higher than from eqFW treatment. It must be noted that the organic material deposition on a flat calcite surface, especially the surface coverage of organic materials, can be different from a rough, porous reservoir rock [16,17].

3.2. In-situ imaging of eqCRO-aged samples

After these preparation steps, we exposed eqCRO-aged samples to pure, 10× and 100× diluted HSW. In pure HSW, eqCRO-aged surfaces hardly change within 24 h (Fig. 2**a and b**) and the observed deposits appear stable for the duration of HSW exposure. Exchanging the ambient brine to 10× diluted HSW changes the picture. After 24 h, the deposit-covered fraction of the surface area decreases to ≈80% of the initial coverage, exposing parts of the hydrophilic calcite directly to the ambient brine. (see Fig. 2**c**). The underlying desorption and/or reorganization of the organic deposits is further accelerated upon exposing the sample to 100× diluted HSW, Fig. 2**d**. The average coverage has decreased to about 40% in 24 h. Moreover, the images display clear signs of etch pits that are characteristic of calcite dissolution as indicated by the arrows in Fig. 2**d** (see also [50,51]). The appearance of dissolution etch pits of calcite indicates that the brine is in direct contact with the original crystalline calcite surface. So, the intermediate modified-calcite must also have been removed by the brine. Chen et al. [41] proposes a model where the modified (i.e. deposited from eqFW-aging) calcite layer, when exposed to diluted brines, detaches readily as flakes which then carries the crude oil and the asphaltenic layer away. But our results show, upon exposure to diluted brines, the decomposition of the PAH-enriched organic layer from eqCRO-aged samples is gradual, at least in field of view explored here. This is not surprising since the eqFW-aged samples (Chen et al.'s 'patchy organic-ionic' layer) and the eqCRO-aged samples are different both chemically and topographically. It should be noted that the eqCRO-aged samples represent surfaces that are present in a real reservoir rock [32,42,43].

3.3. In-situ imaging of eqFW-aged samples

To definitively demonstrate that the responses of eqFW-aged samples are distinct from eqCRO-aged samples, we tracked the surface evolution of eqFW-aged samples in HSW and its dilutions separately. As shown in Fig. 3 the modified-calcite layer is relatively stable in HSW in the time span of measurement (**Figure S2**). However, when exposed to 10xdiluted HSW, the modified-calcite layer started dissolving immediately (Fig. 3**b**) and within 2 h, almost 50% of the deposits have dissolved (Fig. 3**c**). After 16 h, we see the characteristic dissolution etch pits of the calcite everywhere on the surface. This once again indicates that the brine is in direct contact with the calcite and hence the modified calcite layer must have been removed in this case as well. However, as expected, the kinetics of dissolution/desorption is different for the eqFW-aged samples and the eqCRO-aged samples under the same brine. For example, with eqFW-aged sample, all deposits have been removed after 16 h in 10xdiluted HSW (Fig. 3**d**) whereas the deposits still remained for the eqCRO-aged sample even after 24 h (Fig. 2**c**). Such observations also indicate that the organic deposits from the eqCRO-aging protect the calcite surface for some time, but then gradually decompose, upon dilution of the ambient brine. In order to identify the microscopic processes related to this gradual decomposition process, we analyzed the mechanical properties of the organic deposits from the same area shown in Fig. 2.

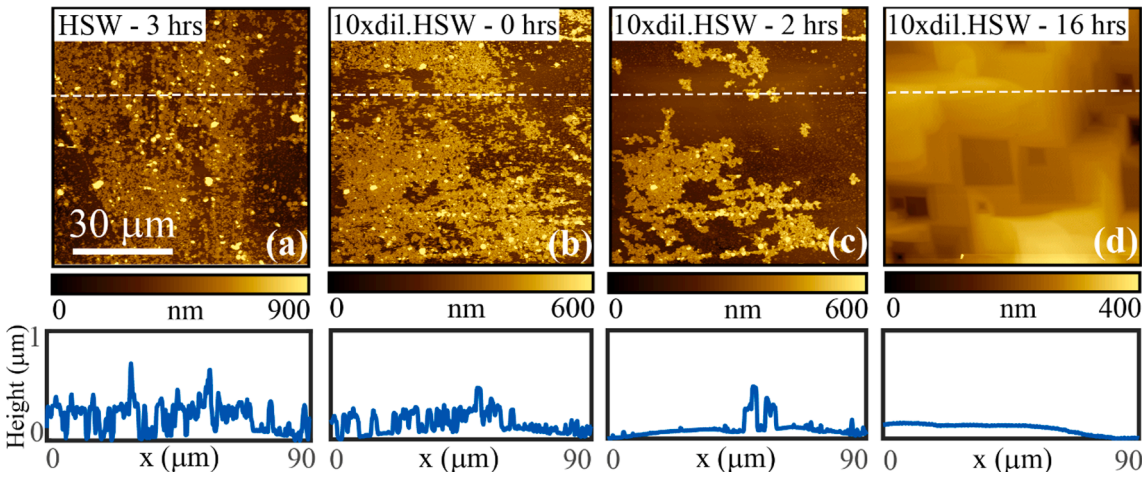

Fig. 3. In-situ AFM topography image of eqFW-aged sample in various dilutions of HSW (Top row – topography; bottom row – cross sections). (a) 3 h in HSW. (b) 0 h in 10xdiluted HSW (c) 2 h in 10xdiluted HSW (d) 16 h in 10xdiluted HSW.

3.4. In-situ mechanical response of crude oil derived organic layers

Fig. 4**a-c** show zoomed views of the same region of the sample from Fig. 2 (white dashed boxes) after subsequent exposure for 24 h to the three different ambient brines as indicated in the figure. First of all, we note that the topography hardly changed between the initial state right after preparation (data not shown) and after 24 h exposure to HSW. At first glance, the morphology after 24 h in 10× diluted HSW appears unaltered. Yet a careful analysis show that the protrusions on the surface do slightly swell, as revealed by the cross sections in Fig. 4**h** along the same location on the surface (white lines in Fig. 4**a, b**). Upon exposure to 100× diluted HSW for 24 h, however, the topography changes dramatically and major parts of the organic deposits have desorbed, also at this specific location on the surface. To characterize the microscopic mechanical response, we recorded force distance curves at every location within these images. Each individual force distance curve consists of an approach curve and a retract curve, as represented schematically in Fig. 4**d** as a function of the displacement of the piezo. In principle, DLVO forces and the adhesion between tip and sample that is measurable upon retraction can be of great interest. However, throughout all our present measurements, the DLVO forces and adhesion turned out to be extremely weak and was therefore not amenable to a detailed analysis (see Fig. 4**e**-g). However, the linear repulsive part of the force at negative values of the piezo displacement revealed interesting information. If

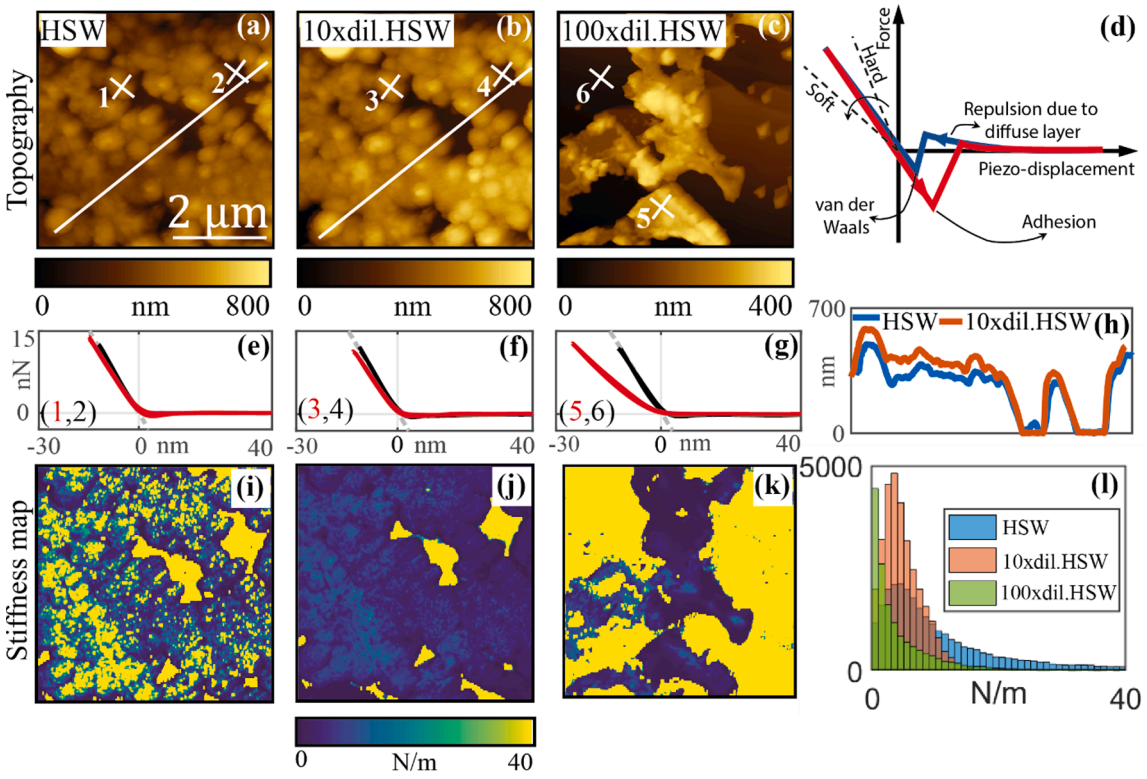

Fig. 4. Topographical and mechanical response of eqCRO-aged sample to various brines. (a)-(c): topography images; (e)-(g): representative force-distance curves taken at the 'x' marks shown in topography maps; (i)-(k): stiffness maps (resolution 256 × 256) corresponding to topography (a) to (c). (d) – A schematic of a typical force-distance curve showing the various force contributions and the slope of constant compliance region for soft and hard materials. (h) – Cross-sections of topography along the line shown in (a) and (b). (l) – Histogram of the stiffness of organic deposits shown in (i)-(k).

the tip is in contact with a perfectly rigid substrate, this part of the curve should have a slope of -k_c. For an elastic substrate, the slope is less steep, as expressed in Eq. (1). Fig. 4**e**-g show force-distance curves at selected locations, labelled as numbers 1–6 in Fig. 4**a-c**. The numbering is chosen such that the odd numbers (red curves) show the response of the organic deposits whereas the even numbers (black curves) show the underlying substrate. Clearly, the stiffness of the organic deposit is close to the one of the substrates in ambient HSW (Fig. 4**e**), slightly softer in 10× diluted HSW (Fig. 4**f**), and substantially softer in 100× diluted HSW (Fig. 4**g**). Fig. 4**i**-k show two-dimensional maps of the same type of data, converted into the local sample stiffness. It should be pointed out that we deliberately refrain from converting the stiffness into an elastic modulus because such a conversion depends strongly on both the exact value of the tip radius and the local thickness of the organic layer. Also, we note here that the stiffness measured is an intrinsic property of the organic material in a given brine and it does not depend on the material or geometry of the AFM tip. The maps reveal that the underlying substrate is indeed very hard with a stiffness exceeding 40 N/m or higher. The substrate stiffness does not change in three different explored ambient brines. Overall, the organic deposits are softer. Only, in ambient HSW, substantial parts of the substrate also reach values beyond 40 N/m (yellow in Fig. 4**i**). These regions become substantially softer with typical stiffness values in the range of 10 N/m in 10× diluted HSW and even softer with typical values below 5 N/m in 100× diluted HSW. Histograms show the evolution of stiffness of eqCRO-derived organic deposits for the various conditions, Fig. 4**l**. It should also be pointed out, that *ex situ* type experiments may not capture these effects.

The observations discussed so far raise the question whether this softening is a signature of the ongoing gradual dissolution process or whether it is an 'intrinsic' equilibrium property of the deposited organic layer. In the latter case, it should be possible to reverse the softening by increasing the salt concentration of ambient brine. In order to check the salinity-dependence of the mechanical response, we measured the stiffness of the eqCRO-aged samples when initially exposed to a 100xdiluted HSW followed by HSW. Fig. 5**a, c, f** shows the response of the eqCRO-aged sample exposed to 100× diluted HSW and Fig. 5**b, d**, g the same area when subsequently exposed to undiluted HSW. The figure panels should be read in the same manner as Fig. 4. The histogram of the stiffness maps (Fig. 5**h**) shows that process is reversible, and the organic deposits indeed become stiffer again upon exposure to HSW. Consistently, cross-sections across the same location (Fig. 5**e**) on the sample show that organic deposits also shrink by several tens of nanometers when exposed to HSW. These observations suggest that the mechanical response of the organic deposits can indeed be interpreted as a salinity-dependent material property. Note that although the quantitative value of the stiffness of the organic deposits in a given brine showed variation across experiments, the qualitative trends were consistent (Figs. 4**l**, 5**h** and **Figure S11**).

4. Discussion

The above observations can be summarized as follows: firstly, the organic materials from eqCRO aging form a protective layer on the calcite surface. Secondly, the stability of this protective layer depends on the salinity of the ambient brine. It is a well-known fact that this layer of organic materials adsorbed on to mineral surface from crude oil is responsible for the oil-wet character of reservoirs [31]. An often-overlooked character is the protective function of these organic materials against mineral dissolution and/or precipitation. Ricci et al. [52] observed even one or two monolayers of steric acid adsorbed onto calcite surfaces slows down the restructuring dynamics of calcite surfaces. In analogous to the solid–liquid electrolyte interphases (SLEI)

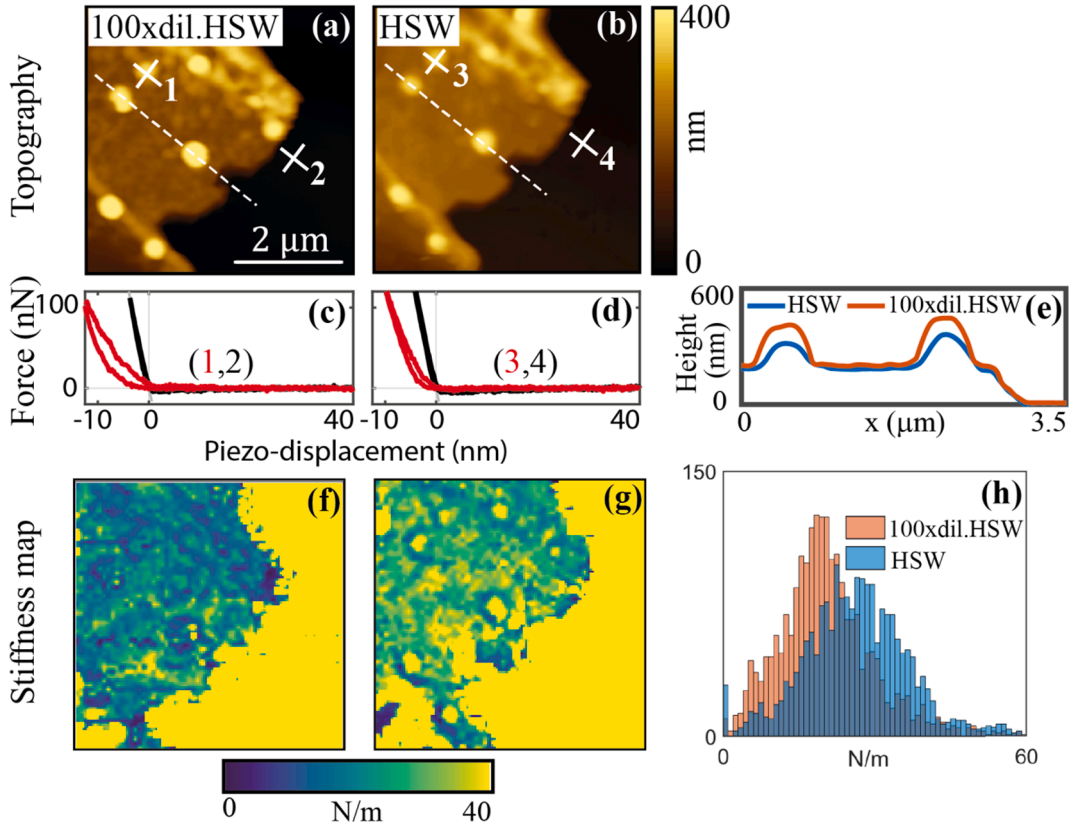

Fig. 5. Reversibility of the mechanical response of the eqCRO-aged sample to brines of variable salinity. (a)-(b): topography images; (c)-(d): representative force-distance curves taken at the 'x' marks shown in topography maps; (f)-(g): stiffness maps (resolution 100 × 100) corresponding to topography (a) and (b); (e) – Cross-sections of topography along the dashed white lines shown in (a) and (b). (h) – Histogram of the stiffness maps shown in (f) and (g).

encountered in semi-solid flow batteries [53,54], we can think of this layer as a 'barrier' for brine to access the mineral surface. But unlike SLEI, the stability of the organic deposits here can be disturbed by changing the salinity of the ambient brine.

The salinity-dependent stability of the organic deposits can be rationalized in the following way: with multiple surface active molecules in crude oil [55–57], the basic unit of PAH-enriched organic deposits is likely a supramolecular assembly of different types of hydrocarbons, with different types of interactions, such as van der Waals, electrostatics, hydration forces, hydrogen bonding, hydrophobic interactions, metal coordination complexes, acid-base interactions, π-π interaction acting between them [58]. These asphaltenes form visco-elastic films at the water–oil interface with that are known to change with time and with the composition of the ambient fluid [59]. The salinity dependence and the gradual response of the stiffness of the crude oil derived organic layers shown in **Figure 4, 5 and S11** are reminiscent of such a behavior. The changes in the visco-elastic properties of the crude-oil derived organic layers are attributed to the rearrangement of molecules at the organic-brine interface due to change in interaction forces [60]. Among the interaction forces, with increasing dilution, van der Waals and hydrophobic interactions are attractive whereas electrostatic interaction, hydration forces can be repulsive, too. Since the organics swell by several tens of nanometers (Fig. 4**h**), we conclude that the changes in the stiffness of the organic layers arise from the change in the magnitude of interaction forces within the organic layer as well and not just at the interface. Swelling of asphaltene aggregates in organic solvents and aqueous solutions has been reported before [39,40,61]. Particularly in aqueous solutions, Abraham et al. [39] showed that the interaction between a silica probe and an asphaltene coated flat silica surface deviated from DLVO behavior and exhibited higher repulsive forces up to 20 nm from the surface in high pH, low (a few mM) KCl concentrations. They attributed this extra repulsive force to steric repulsion between swollen or stretched surface asphaltenes and the silica probe. Here, a similar mechanism can be at play where the affinity of organic deposits for solvent molecules (i.e., water) increases upon brine dilution. This increased affinity changes the balance of forces between asphaltene molecules within the organic layer and possibly with underlying substrate thereby leading to swelling, softening and desorption. The increased affinity of PAH molecules to diluted salt solutions (compared to high-saline brines) could be due to the 'salting-out' effect that was first introduced by Hoffmeister in the context salt-dependent protein solubility [62,63]. The effect describes the decrease in solubility of a non-electrolyte with increasing the salinity of the ambient aqueous solvent [64]. 'Salting-out' is also well-documented for petroleum asphaltenes [65–67]. There are many competing theories for the exact mechanism behind the salting-out effect [64]. In simple terms, it can be explained as follows: At high salt concentration, the ions in the brine remain strongly hydrated/solvated and the interactions between solvent molecules and the organic molecules are weak. This increases the interaction among organic molecules which leads to aggregation. Upon decreasing the salt concentration, the competition between salt ions and organic molecules for water molecules decreases. Therefore, more water molecules solvate the organic molecules and increase its solubility (Fig. 6). Since increased oil recovery is always observed below a certain critical salinity, salting-out effect has been proposed to be one of the mechanisms behind LSE for sandstone reservoirs [10]. Austad et al. [68] tested this hypothesis by studying adsorption of model organic molecules onto kaolinite particles. Salting-out effects was found to contribute to LSE especially if the organic material that makes the mineral oil-wet contains carboxylates/

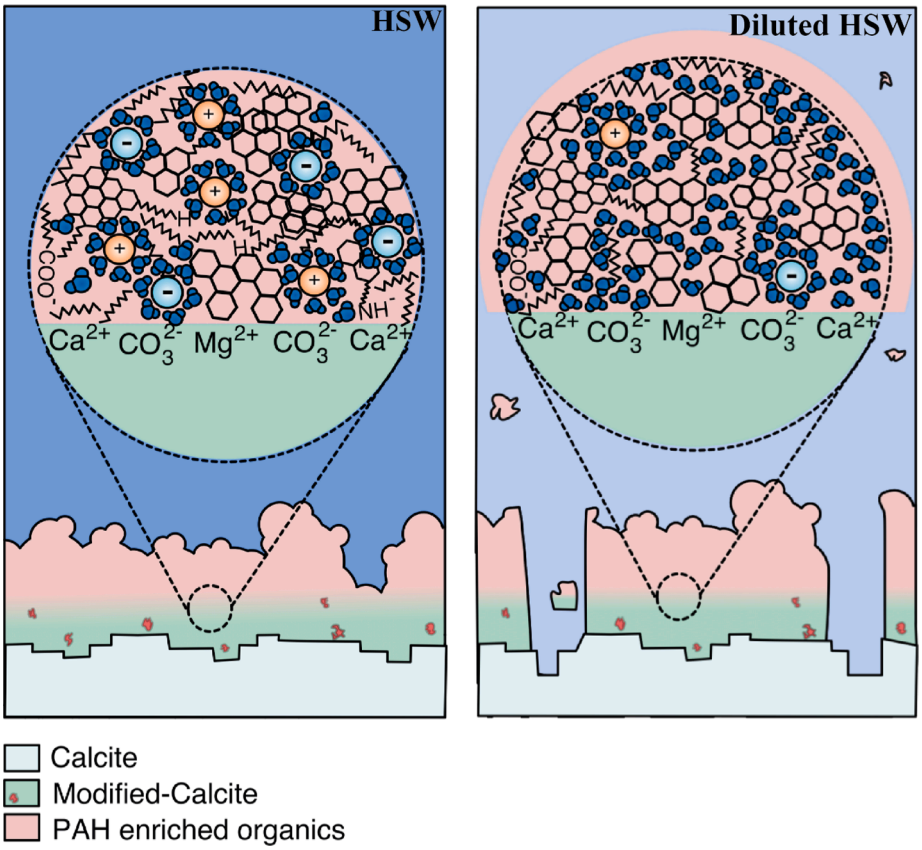

Fig. 6. A schematic of the proposed mechanism, where PAH-enriched organic layer swells in diluted brine and the ions in the diluted brine change the interaction between organic molecules and between the organic molecules and the mineral surface. This causes the organic materials to desorb and exposes the calcite substrate to the diluted brine leading to mineral dissolution.

carboxylic acids. However, for carbonate reservoirs, it was argued that the salting-out effect cannot contribute to LSE owing to strong adsorption of carboxylic materials on to the calcite surface. But this argument overlooks two important factors. Firstly, there is multi-layer adsorption of organic materials on to the calcite surface [31,32]. So, the intermolecular interactions between the organic molecules are as important as the interactions between the calcite surface and the organic molecules. Desorption of organic molecules can be brought about by changing the interactions between organic molecules. Secondly, the organic materials from eqCRO adsorb on to the newly reconstructed modified calcite layer and not the pristine calcite surface. The first point is evident from the swelling and softening of organic deposits upon exposure to diluted brines (Fig. 4). Moreover, the fact that the vast majority of organic deposits is removed from the surfaces in our experiments in diluted brines clearly shows that, at least, not all organic deposits are strongly adsorbed to the modified calcite surface. One could argue that the removal of organic deposits from the calcite surface is due to mineral dissolution rather than salting-out effects.

While our data do indeed show mineral dissolution in diluted brines, it is clear that swelling and desorption of organic deposits take place before the first indications of mineral dissolution (Fig. 2**b**). Salting-out effects thus precede mineral dissolution. Hence, the removal of organic deposits is triggered by the increased water affinity in diluted brines and subsequently possibly enhanced by mineral dissolution.

One might attribute the swelling of organic deposits in low-salinity brines to the repulsive interaction between the asphaltenes due to their electric double layer in aqueous solution. However, the calculated Debye length for 10xdil. HSW is less than 1 nm. At such short distances, steric effects due to finite ion sizes, short-range hydration forces, van der Waals forces and electric double layer forces are all intertwined and classical Poisson-Boltzmann theory generally fails [69]. A description of the swelling of organic deposits (Fig. 4**h**) in 10xdil. HSW in terms of double layer forces following DLVO theory is therefore not justified. Only in 100xdil. HSW with a Debye length of ≈2.89 nm classical electrical double layer forces can be expected to emerge as a clear separate contribution in the overall molecular forces and thereby provide an independent contribution to the swelling of asphaltenes. It should be pointed out, however, that 100xdil. HSW is much less saline than any common injection water.

In carbonate reservoirs, whose wettability ranges from mixed-wet to oil-wet, the ultimate recovery by low-salinity IOR depends on a multitude of physical mechanisms that take place over several length scales at both mineral-brine and oil-brine interfaces. For any mechanism such as dissolution and multi-component ion exchange to occur at the mineral surface, the ions and solvent molecules from the brine have to cross the barrier of adsorbed organic layers. Hence de-stabilizing the organic layer either by desorption or swelling becomes a prerequisite for any IOR mechanisms at the mineral-brine interface. This suggests that salting-out effects mostly likely contribute either directly or indirectly to the desorption of organic layers from the carbonate surfaces. Note, however, that these layers are not purely organic but contain a complex mixture of 'modified calcite' (see Fig. 6) involving both adsorbed organics and co-adsorbed/precipitated carbonate mineral [31]. The desorption of this layer upon exposure to brines of reduced salinity thus suggests a combined effect of organic and mineral dissolution, which should be unique to carbonate reservoirs. We stress, however, that the salting-out effect in itself is not specific to carbonate surfaces. For example, Haagh et al. [33] observed similar softening of (carbonate-free) crude-oil deposits on mica surfaces upon exposure to low-salinity brines.

It has also been argued that the roughness of surfaces could play an important role for the oil release. Compared to actual porous rocks, our cleaved calcite surfaces are much flatter. Roughness probably affects the adhesion of the precipitated organic and modified calcite layers on the substrate. Very flat substrates may lead to reduced adhesion and thereby promote the detachment of larger pieces, as reported by Chen et al. [41], which would be less likely to occur in a random porous medium. The softening and salt-outing effect described in this work, however, takes place on the molecular scale. Therefore, we expect that it should be equally relevant in a more complex porous medium as on our flat substrates.

Finally, we would like to concede that we are unable to estimate the quantitative relevance of our observations for enhanced oil recovery. The overall recovery factor involves processes on multiple length scales and there are currently no reliable tools available to bridge these scales to obtain reliable quantitative predictions. Nevertheless, the softening and enhanced dissolution of organic layers should take place in actual oil reservoirs – albeit perhaps in a somewhat modified manner due to the elevated temperatures and pressures. Hence, we definitely expect that these processes will contribute to rendering oil-wet and mixed-wet reservoirs more water-wet and should thereby contribute to an enhanced recovery [28,70].

5. Conclusion

Our results highlight the various intermediate processes that take place during the modification of oil-wet/mixed-wet calcite surfaces to water-wet upon exposure to low-salinity brines. The adsorbed organic layer from crude oil responsible for the oil-wetness of the reservoir rocks also act as a barrier for the ions to access the mineral surface. Most low-salinity IOR strategies for carbonate reservoirs target the mineral-brine interface by optimizing the composition of potential-determining ions. But our results show that the mineral surface is essentially inaccessible by any such ions unless the barrier by organic materials is overcome. The stability of the organic layer is found to be disturbed by lowering the salinity of ambient brines. This phenomenon can be explained in terms of 'salting-out' effects. The existence and the salinity-dependent stability of this organic layer has major implications for any IOR strategy that targets the brine-mineral interface or the brine-oil interface.

In summary, our results show a new pathway to increase the water-wetness of calcite mineral surfaces by targeting the protective organic layer via 'salting-out' effect. Future experiments involving ions from the Hoffmeister series in the low salinity brines might help to prove this strategy even more strongly.

CRediT authorship contribution statement

Saravana Kumar: Conceptualization, Data curation, Investigation, Writing - review & editing. **Ashit Rao:** Investigation, Writing - review & editing. **Mohammed B. Alotaibi:** Writing - review & editing. **Subhash C. Ayirala:** Writing - review & editing. **Ali A. Yousef:** Writing - review & editing. **Igor Siretanu:** Conceptualization, Supervision, Writing - review & editing. **Frieder Mugele:** Conceptualization, Supervision, Writing - review & editing.

Declaration of Competing Interest

The authors declare that they have no known competing financial interests or personal relationships that could have appeared to influence the work reported in this paper.

Acknowledgements

We thank Carla Annink for her help in the preparation of aged samples used for AFM topography imaging and mechanical characterization experiments reported in this study. Funding from the Saudi Arabian Oil Company (Saudi Aramco) under the contract no. 6600041100 is gratefully acknowledged.

Appendix A. Supplementary data

Supplementary data to this article can be found online at https://doi.

org/10.1016/j.fuel.2021.121129.

References

[1] Bernard GG. Effect of floodwater salinity on recovery of oil from cores containing clays. in SPE California Regional Meeting. 1967. Society of Petroleum Engineers.
[2] Morrow N, Buckley J. Improved oil recovery by low-salinity waterflooding. J Petrol Technol 2011;63(05):106–12.
[3] Morrow NR, Tang G-Q, Valat M, Xie X. Prospects of improved oil recovery related to wettability and brine composition. J Petrol Sci Eng 1998;20(3-4):267–76.
[4] Tang G, Morrow NR. Salinity, temperature, oil composition, and oil recovery by waterflooding. SPE Reservoir Eng 1997;12(04):269–76.
[5] Tang G-Q, Morrow NR. Influence of brine composition and fines migration on crude oil/brine/rock interactions and oil recovery. J Petrol Sci Eng 1999;24(2-4):99–111.
[6] Sheng JJ. Critical review of low-salinity waterflooding. J Petrol Sci Eng 2014;120:216–24.
[7] Lager A, et al. Low salinity oil recovery-an experimental investigation1. Petrophysics 2008;49(01).
[8] Buckley J, Morrow N. Improved oil recovery by low salinity waterflooding: a mechanistic review. 11th international symposium on evaluation of wettability and its effect on oil recovery. 2010.
[9] Ligthelm DJ et al. Novel Waterflooding Strategy By Manipulation Of Injection Brine Composition. in EUROPEC/EAGE conference and exhibition. 2009. Society of Petroleum Engineers.
[10] RezaeiDoust A, Puntervold T, Strand S, Austad T. Smart water as wettability modifier in carbonate and sandstone: a discussion of similarities/differences in the chemical mechanisms. Energy Fuels 2009;23(9):4479–85.
[11] Al-sofi AM, Yousef AA. Insight into smart-water recovery mechanism through detailed history matching of coreflood experiments. in SPE Reservoir Characterization and Simulation Conference and Exhibition. 2013. Society of Petroleum Engineers.
[12] McGuire P et al. Low salinity oil recovery: An exciting new EOR opportunity for Alaska's North Slope. In SPE western regional meeting. 2005. Society of Petroleum Engineers.
[13] Haagh MEJ, Schilderink N, Mugele F, Duits MHG. Wetting of mineral surfaces by fatty-acid-laden oil and brine: carbonate effect at elevated temperature. Energy Fuels 2019;33(10):9446–56.
[14] Haagh MEJ, Siretanu I, Duits MHG, Mugele F. Salinity-dependent contact angle alteration in oil/brine/silicate systems: the critical role of divalent cations. Langmuir 2017;33(14):3349–57.
[15] Bera B, Kumar N, Duits MHG, Cohen Stuart MA, Mugele F. Cationic hofmeister series of wettability alteration in mica–water–alkane systems. Langmuir 2018;34(45):13574–83.
[16] Rücker M, Bartels W-B, Garfi G, Shams M, Bultreys T, Boone M, et al. Relationship between wetting and capillary pressure in a crude oil/brine/rock system: From nano-scale to core-scale. J Colloid Interface Sci 2020;562:159–69.
[17] Rücker M, et al. Workflow for upscaling wettability from the nanoscale to core scale. Petrophysics 2020;61(02):189–205.
[18] Mohammadi M, Mahani H. Direct insights into the pore-scale mechanism of low-salinity waterflooding in carbonates using a novel calcite microfluidic chip. Fuel 2020;260:116374.
[19] Xie Y, Khishvand M, Piri M. Impact of connate brine chemistry on in situ wettability and oil recovery: pore-scale experimental investigation. Energy Fuels 2020;34(4):4031–45.
[20] Blunt MJ, Multiphase flow in permeable media: A pore-scale perspective. 2017: Cambridge University Press.
[21] Bartels W-B, Mahani H, Berg S, Hassanizadeh SM. Literature review of low salinity waterflooding from a length and time scale perspective. Fuel 2019;236:338–53.
[22] Hilner E, Andersson MP, Hassenkam T, Matthiesen J, Salino PA, Stipp SLS. The effect of ionic strength on oil adhesion in sandstone–the search for the low salinity mechanism. Sci Rep 2015;5(1). https://doi.org/10.1038/srep09933.
[23] Zhang P, Tweheyo MT, Austad T. Wettability alteration and improved oil recovery by spontaneous imbibition of seawater into chalk: impact of the potential determining ions Ca2+, Mg2+, and SO42−. Colloids Surf, A 2007;301(1–3):199–208.
[24] Amott E. Observations relating to the wettability of porous rock. Trans AIME 1959;216(01):156–62.
[25] Mahani H, Keya AL, Berg S, Bartels W-B, Nasralla R, Rossen WR. Insights into the mechanism of wettability alteration by low-salinity flooding (LSF) in carbonates. Energy Fuels 2015;29(3):1352–67.
[26] Valvatne PH, Blunt MJ. Predictive pore-scale modeling of two-phase flow in mixed wet media. Water Resour Res 2004;40(7). https://doi.org/10.1029/2003WR002627.
[27] Vledder P, et al. Low salinity water flooding: proof of wettability alteration on a field wide scale. In SPE Improved Oil Recovery Symposium. 2010. Society of Petroleum Engineers.
[28] Yousef AA, et al., Laboratory investigation of the impact of injection-water salinity and ionic content on oil recovery from carbonate reservoirs. SPE Reservoir Evaluation & Engineering, 2011. 14(05): p. 578-593.
[29] Akbar M et al., A snapshot of carbonate reservoir evaluation. Oilfield Review, 2000. 12(4): p. 20-21.
[30] Strand S, Høgnesen EJ, Austad T. Wettability alteration of carbonates—effects of potential determining ions (Ca2+ and SO42−) and temperature. Colloids Surf, A 2006;275(1-3):1–10.
[31] Rao A, Kumar S, Annink C, Le-Anh D, Ayirala SC, Alotaibi MB, et al. Mineral interfaces and oil recovery: a microscopic view on surface reconstruction, organic modification and wettability alteration of carbonates. Energy Fuels 2020;34(5):5611–22.
[32] Rao A et al., Artificial Diagenesis of Carbonates: Temperature-Dependent Inorganic and Organic Modifications in Reservoir Mimetic Fluids. SPE Journal, 2020.
[33] Haagh M, et al. Aging brine-dependent deposition of crude oil components onto mica substrates, and its consequences for wettability. Fuel 2020;274:117856.
[34] Buckley JS, Liu Y. Some mechanisms of crude oil/brine/solid interactions. J Petrol Sci Eng 1998;20(3-4):155–60.
[35] Drummond C, Israelachvili J. Fundamental studies of crude oil–surface water interactions and its relationship to reservoir wettability. J Petrol Sci Eng 2004;45(1-2):61–81.
[36] Tessarolo N, Wang N, Wicking C, Collins I, Webb K, Couves J, et al. Identification of organic species with "double-sided tape" characteristics on the surface of carbonate reservoir rock. Fuel 2021;288:119627. https://doi.org/10.1016/j.fuel.2020.119627.
[37] Natarajan A, Xie J, Wang S, Masliyah J, Zeng H, Xu Z. Understanding molecular interactions of asphaltenes in organic solvents using a surface force apparatus. J Phys Chem C 2011;115(32):16043–51.
[38] Wang S, Liu J, Zhang L, Masliyah J, Xu Z. Interaction forces between asphaltene surfaces in organic solvents. Langmuir 2010;26(1):183–90.
[39] Abraham T, et al. Asphaltene− silica interactions in aqueous solutions: direct force measurements combined with electrokinetic studies. Ind Eng Chem Res 2002;41(9):2170–7.
[40] Campen SM, Moorhouse SJ, Wong JSS. Effect of aging on the removal of asphaltene deposits with aromatic solvent. Langmuir 2019;35(37):11995–2008.
[41] Chen S-Y, Kaufman Y, Kristiansen K, Seo D, Schrader AM, Alotaibi MB, et al. Effects of salinity on oil recovery (the "Dilution Effect"): experimental and theoretical studies of crude oil/brine/carbonate surface restructuring and associated physicochemical interactions. Energy Fuels 2017;31(9):8925–41.
[42] Ivanova A, Mitiurev N, Cheremisin A, Orekhov A, Kamyshinsky R, Vasiliev A. Characterization of organic layer in oil carbonate reservoir rocks and its effect on microscale wetting properties. Sci Rep 2019;9(1). https://doi.org/10.1038/s41598-019-47139-y.
[43] Ivanova A et al. Microstructural Imaging and Characterization of Organic Matter Presented in Carbonate Oil Reservoirs. In SPE Europec featured at 81st EAGE Conference and Exhibition. 2019. Society of Petroleum Engineers.
[44] Ayirala S, et al. Linking pore scale mechanisms with macroscopic to core scale effects in controlled ionic composition low salinity waterflooding processes. Fuel 2020;264:116798.
[45] Fenter P, Qin T, Lee SS, AlOtaibi MB, Ayirala S, Yousef AA. Molecular-scale origins of wettability at petroleum–brine–carbonate interfaces. Sci Rep 2020;10(1). https://doi.org/10.1038/s41598-020-77393-4.
[46] Hutter JL, Bechhoefer J. Calibration of atomic-force microscope tips. Rev Sci Instrum 1993;64(7):1868–73.
[47] Cappella B, Dietler G. Force-distance curves by atomic force microscopy. Surf Sci Rep 1999;34(1-3):1–104.
[48] Stipp SLS, Gutmannsbauer W, Lehmann T. The dynamic nature of calcite surfaces in air. Am Mineral 1996;81(1-2):1–8.
[49] Borromeo L, Zimmermann U, Andò S, Coletti G, Bersani D, Basso D, et al. Raman spectroscopy as a tool for magnesium estimation in Mg-calcite. J Raman Spectrosc 2017;48(7):983–92.
[50] Hillner PE, Gratz AJ, Manne S, Hansma PK. Atomic-scale imaging of calcite growth and dissolution in real time. Geology 1992;20(4):362.
[51] Hillner PE, Manne S, Gratz AJ, Hansma PK. AFM images of dissolution and growth on a calcite crystal. Ultramicroscopy 1992;42-44:1387–93.
[52] Ricci M, Segura JJ, Erickson BW, Fantner G, Stellacci F, Voïtchovsky K. Growth and dissolution of calcite in the presence of adsorbed stearic acid. Langmuir 2015;31(27):7563–71.
[53] Busche MR, Drossel T, Leichtweiss T, Weber DA, Falk M, Schneider M, et al. Dynamic formation of a solid-liquid electrolyte interphase and its consequences for hybrid-battery concepts. Nat Chem 2016;8(5):426–34.
[54] Narayanan A, Wijnperlé D, Mugele F, Buchholz D, Vaalma C, Dou X, et al. Influence of electrochemical cycling on the rheo-impedance of anolytes for Li-based Semi Solid Flow Batteries. Electrochim Acta 2017;251:388–95.
[55] Mullins OC, Betancourt SS, Cribbs ME, Dubost FX, Creek JL, Andrews AB, et al. The colloidal structure of crude oil and the structure of oil reservoirs. Energy Fuels 2007;21(5):2785–94.
[56] Marshall AG, Rodgers RP. Petroleomics: chemistry of the underworld. Proc Natl Acad Sci 2008;105(47):18090–5.
[57] Beens J, Blomberg J, Schoenmakers PJ. Proper tuning of comprehensive two-dimensional gas chromatography (GC× GC) to optimize the separation of complex oil fractions. J High Resolut Chromatogr 2000;23(3):182–8.
[58] Gray MR, Tykwinski RR, Stryker JM, Tan X. Supramolecular assembly model for aggregation of petroleum asphaltenes. Energy Fuels 2011;25(7):3125–34.
[59] Adams JJ. Asphaltene adsorption, a literature review. Energy Fuels 2014;28(5):2831–56.
[60] Langevin D, Argillier J-F. Interfacial behavior of asphaltenes. Adv Colloid Interface Sci 2016;233:83–93.
[61] Nikooyeh K, Bagheri SR, Shaw JM. Interactions between Athabasca pentane asphaltenes and n-alkanes at low concentrations. Energy Fuels 2012;26(3):1756–66.
[62] Hofmeister F. Zur lehre von der wirkung der salze. Archiv für experimentelle Pathologie und Pharmakologie 1888;25(1):1–30.

[63] Kunz W, Henle J, Ninham BW. 'Zur Lehre von der Wirkung der Salze'(about the science of the effect of salts): Franz Hofmeister's historical papers. Curr Opin Colloid Interface Sci 2004;9(1-2):19–37.
[64] Grover PK, Ryall RL. Critical appraisal of salting-out and its implications for chemical and biological sciences. Chem Rev 2005;105(1):1–10.
[65] Hamam SM, Hamoda MohamedF, Shaban HabibI, Kilani AmalS. Crude oil dissolution in saline water. Water Air Soil Pollut 1988;37(1-2). https://doi.org/10.1007/BF00226479.
[66] Price LC. Aqueous solubility of petroleum as applied to its origin and primary migration. AAPG Bull 1976;60(2):213–44.
[67] Standal SH, Blokhus AM, Haavik J, Skauge A, Barth T. Partition coefficients and interfacial activity for polar components in oil/water model systems. J Colloid Interface Sci 1999;212(1):33–41.
[68] Austad T, RezaeiDoust A, Puntervold T. Chemical mechanism of low salinity water flooding in sandstone reservoirs. in SPE improved oil recovery symposium. 2010. Society of Petroleum Engineers.
[69] Ben-Yaakov D, et al. Beyond standard Poisson-Boltzmann theory: ion-specific interactions in aqueous solutions. J Phys: Condens Matter 2009;21(42):424106.
[70] Yousef A, et al., SmartWater Flooding: Industry's First Field Test in Carbonate Reservoirs, SPE-159526 presented at the SPE Annual Technical Conference and Exhibition held in San Antonio, Texas, USA, 8–10 October. 2012.